JOURNAL OF MATERIALS SCIENCE **21** (1986) 4245–4249

Structural analysis of amorphous $(Fe_{1-x}Mn_x)_{78}B_{22}$ alloys by X-ray diffraction and electrical resistance

TETSUO SOUMURA, SHIGERU SAITO, KENICHIRO TAKEDA, TAKAO MAEDA
Department of Electrical Engineering, Science University of Tokyo, Kagurazaka, Shinjuku-ku, Tokyo 162, Japan

The structure of amorphous $(Fe_{1-x}Mn_x)$ alloys prepared by a single roller technique has been investigated in terms of X-ray diffraction and electrical resistance. The lattice parameter of the crystalline precipitates, which were α-Fe and bct $(FeMn)_3B$, was determined under different heat treatments. On heating up to 440° C where a mixture of amorphous and crystalline phases exists and up to 550° C corresponding to the completion of crystallization, the lattice parameter of the α-Fe phase rises to that of pure α-Fe with increasing manganese concentration. In samples annealed at 660° C for 5 h, the opposite behaviour is observed. These results can be explained on the basis of the position of the boron atom occupying the α-Fe lattice, the pressure effect exerted by the environment, and the enhancement of the chemical short-range ordering between manganese and boron atoms with manganese concentration. In the bct phase, which shows a reduction in lattice parameter with manganese concentration independent of heat treatment, the effect of redistribution of the atoms in the unit cell should be also taken into account.

1. Introduction

Iron-based amorphous alloys are of great fundamental and technical interest. For instance, in contrast to Fe–B alloys which are ferromagnetic in the amorphous state, ternary Fe–B alloys containing manganese atoms exhibit a characteristic magnetic behaviour, i.e. transition from ferromagnetism to spin glass phase at a critical manganese concentration due to increasing antiferromagnetic coupling between manganese atoms with manganese concentration [1–5]. The crystallization process, which has a significant effect on the change in physical properties, has been extensively investigated. In binary Fe–B alloys, the precipitate formed on crystallization is α-Fe and, depending on the alloy composition and the heat treatment, metastable bct or orthorhombic Fe_3B compound is produced and the equilibrium state is the mixture of α-Fe and bct Fe_2B phases [6–8]. In ternary Fe–B alloys with a manganese atom substituted for an iron atom, the bct $(FeMn)_3B$ phase which appears is reported to be the metastable phase [9]. However, more detailed knowledge is required about the change in structure caused by manganese atoms added to binary Fe–B alloys during the crystallization process.

The present work is mainly concerned with the stucture analysis of crystallization products under different heat treatments in connection with the temperature dependence of electrical resistance for ternary $(Fe_{1-x}Mn_x)_{78}B_{22}$ alloys. In addition, the variation of electrical resistance during the crystallization process as a function of temperature and manganese concentration up to $x = 0.20$ is discussed. Discussion is also presented of the structure of the precipitates formed on crystallization, taking into account position of the boron atom.

2. Experimental procedure

Amorphous $(Fe_{1-x}Mn_x)_{78}B_{22}$ alloys were prepared by quenching ingots arc-melted in an argon atmosphere by means of a single roller technique with a roller diameter of 15 cm and a revolution of 6000 r.p.m. The electron-beam method was applied to melt the ingots in a vacuum of 10^{-4} torr (1.33×10^{-2} Pa), which serves to decontaminate the samples and to reduce mixing of impurities. The amorphous state of the samples was identified by X-ray diffraction using Cu$K\alpha$ radiation. The electrical resistance was measured by a d.c. four-probe method at heating rates of 2 and 10° C min^{-1} over the temperature range 0 to 700° C. The change in crystal structure during the crystallization process was examined by X-ray diffraction under the following three types of heat treatment with reference to the data of resistance: (1) heating to 433 to 440° C, where the alloys consist of a mixture of amorphous phase and crystalline phase; (2) heating to 510 to 550° C, which is the temperature corresponding to completion of crystallization as shown in Fig. 1 as T_L; and (3) annealing at 660° C for 5 h, where only the crystalline phase exists. In Conditions 1 and 2, the samples were successively cooled to room temperature not more than 40 sec after being heated to the specified temperature at a heating rate of 2° C min^{-1}, to impede the progress of crystallization.

0022–2461/86 $03.00 + .12

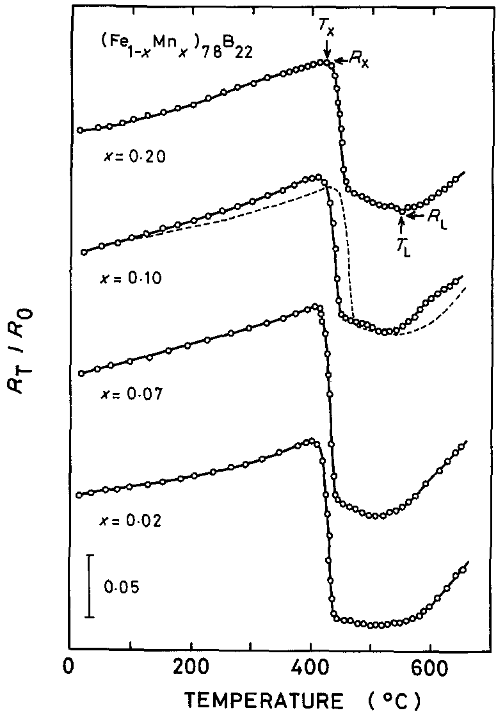

Figure 1 Temperature dependence of electrical resistance at a heating rate of 2° C min^{-1} for $(Fe_{1-x}Mn_x)_{78}B_{22}$ alloys where the resistance is normalized to that at room temperature. The dashed line is a curve at 10° C min^{-1}.

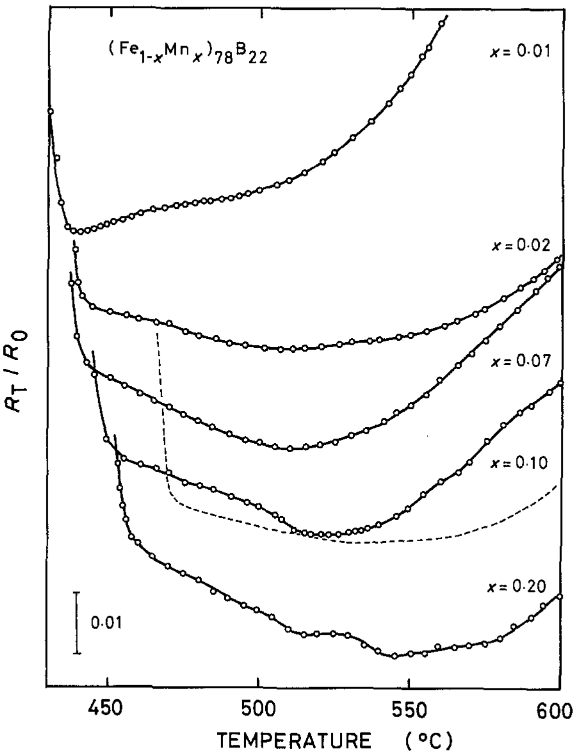

Figure 2 Change in resistance, displayed on an enlarged scale, during the crystallization process in Fig. 1. Heating rate: (○—○) 2° C min^{-1}, (– – –) 10° C min^{-1}.

3. Results

3.1. Electrical resistance

Fig. 1 shows the temperature dependence of electrical resistance at a heating rate of 2° C min^{-1} for $(Fe_{1-x}Mn_x)_{78}B_{22}$ alloys. The crystallization temperature, T_x, is defined as the temperature at which the resistance begins to drop drastically. It is found that T_x increases slightly with manganese concentration. The characteristic variation of resistance with temperature is observed during the crystallization process as the manganese concentration increases. In Fig. 2, the behaviour of resistance near T_x and above, is displayed on an enlarged scale. For a manganese concentration $x = 0.01$, we can see that there is an increase in resistance with temperature just after an abupt decrease in resistance. With increasing manganese concentration, on the other hand, the resistance gradually decreases in the latter half of the crystallization process, followed by a distinct resistance minimum which shifts to the higher temperature side. The quantitative variation mentioned above is given in Fig. 3 at heating rates of 2 and 10° C min^{-1}, where T_L is the temperature at the resistance minimum, and R_L and R_x are the resistances at T_L and T_x, respectively, as shown in Fig. 1. The resistance difference, $R_x - R_L$, decreases with manganese concentration and the temperature difference, $T_L - T_x$, increases. This results in the amorphous–crystalline transition becoming more obscure in alloys with higher manganese concentrations.

3.2. X-ray diffraction

The X-ray diffraction patterns on the low angle side near the first halo peak are shown for $x = 0.10$ in Fig. 4 under the three heat treatments. A peak of α-Fe (1 1 0) is observed near $2\theta = 45°$, with other peaks for the Miller indices quoted in the figure corresponding to the b c t phase which is considered to be $(FeMn)_3B$. A sharp and enhanced peak is seen for α-Fe (1 1 0) upon heating at high temperatures and long-term annealing. However, the tendency does not necessarily follow for b c t phase, because the intensity of the

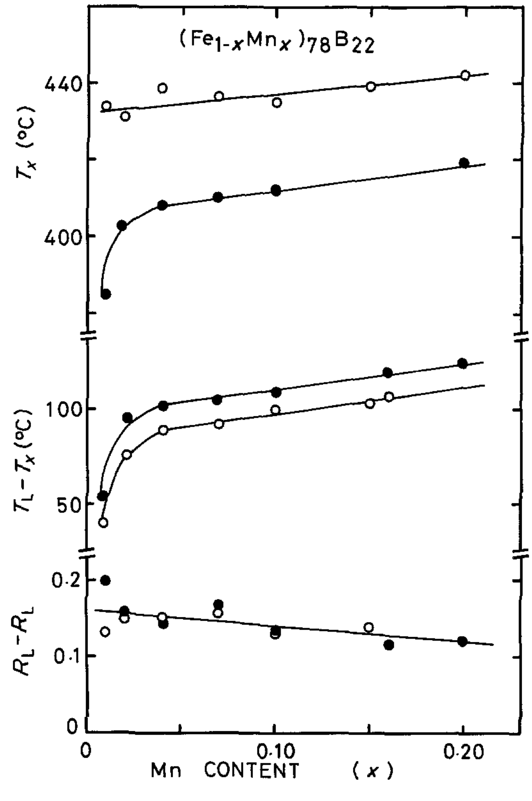

Figure 3 Manganese concentration dependence of T_x, $T_L - T_x$ and $R_x - R_L$. Heating rates: (○) 10° C min^{-1}, (●) 2° C min^{-1}.

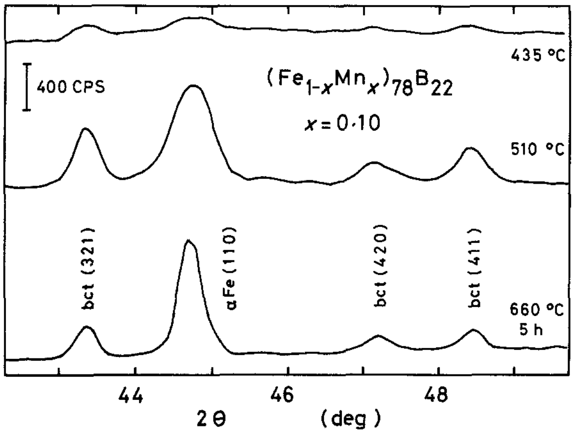

Figure 4 X-ray diffraction patterns near the first halo peak for $(Fe_{0.9}Mn_{0.1})_{78}B_{22}$ alloy under three heat treatments.

TABLE I X-ray diffraction data for $(Fe_{0.9}Mn_{0.1})_{78}B_{22}$ alloy for the three heat treatments. The observed intensity I_{obs} is normalized to the maximum in each structure

hkl	d_{obs} (nm)	d_{cal} (nm)	I_{obs}	Str.
(1) *Heating to 435° C*				
3 2 1	0.2078	0.2086	100	b c t
1 1 0	0.2017	0.2024	100	α-Fe
4 2 0	0.1919	0.1920	34	b c t
4 1 1	0.1871	0.1876	72	b c t
5 1 0	0.1682	0.1684	31	b c t
6 1 1	0.1344	0.1342	13	b c t
3 1 0	0.0906	0.0906	19	α-Fe
(2) *Heating to 510° C*				
4 0 0	0.2141	0.2151	14	b c t
3 2 1	0.2085	0.2085	100	b c t
1 1 0	0.2024	0.2026	100	α-Fe
4 2 0	0.1923	0.1923	36	b c t
4 1 1	0.1877	0.1877	59	b c t
2 2 2	0.1751	0.1753	16	b c t
5 1 0	0.1685	0.1687	25	b c t
2 0 0	0.1434	0.1433	8	α-Fe
6 1 1	0.1344	0.1343	11	b c t
5 5 0	0.1219	0.1217	17	b c t
6 4 0	0.1197	0.1193	8	b c t
2 1 1	0.1173	0.1170	11	α-Fe
0 0 4	0.1068	0.1072	7	b c t
5 5 2	0.1060	0.1058	7	b c t
2 2 0	0.1015	0.1013	4	α-Fe
3 1 0	0.0908	0.0906	2	α-Fe
(3) *Annealing at 660° C for 5 h*				
4 0 0	0.2152	0.2152	13	b c t
3 2 1	0.2090	0.2088	100	b c t
1 1 0	0.2026	0.2027	100	α-Fe
4 2 0	0.1927	0.1926	43	b c t
4 1 1	0.1879	0.1879	52	b c t
2 2 2	0.1754	0.1756	17	b c t
3 1 2	0.1688	0.1688	30	b c t
2 0 0	0.1429	0.1433	10	α-Fe
5 5 0	0.1218	0.1218	11	b c t
2 1 1	0.1174	0.1171	11	α-Fe
2 2 0	0.1014	0.1014	4	α-Fe
3 1 0	0.0908	0.0907	6	α-Fe

Heat treatment	Lattice parameter (nm)		
	α-Fe *a*	b c t *a*	b c t *c*
(1)	0.2863	0.8587	0.4323
(2)	0.2865	0.8604	0.4290
(3)	0.2867	0.8611	0.4302

peaks rather diminishes on annealing at 660° C for 5 h. In Table I, the X-ray diffraction data for the same alloy are collected.

The lattice parameter of the b c t $(FeMn)_3B$ phase is given in Fig. 5 as a function of manganese concentration for the three heat treatments. The features are summarized as follows: (1) the heat treatment has an insignificant influence on the lattice parameter in manganese-enriched alloys; (2) the manganese concentration dependence of the lattice parameter is remarkable, especially on heating to 433 to 440° C; and (3) the lattice parameter of the annealed samples (660° C, 5 h) is large compared to that of those heated to 510 to 550° C.

Fig. 6 shows the variation of lattice parameter for the α-Fe phase with manganese concentration and heat treatment. With increasing manganese concentration the lattice parameter approaches that of pure α-Fe in any heat treatment. However, it should be noted that the lattice subject to annealing at 660° C for 5 h expands, compared to the pure α-Fe lattice subjected to other heat treatments.

4. Discussion

4.1. Electrical resistance

In general, it is proved that the coexistence of the crystalline phase in an amorphous matrix leads to a decrease in T_x [10]. As seen in Fig. 3, however, T_x increases slightly with manganese concentration. The manganese concentration dependence of T_x, therefore, may be interpreted on the assumption that the presence of a manganese atom gives rise to a delay in the amorphous–crystalline transition for the following reasons: in a locally manganese-rich region in

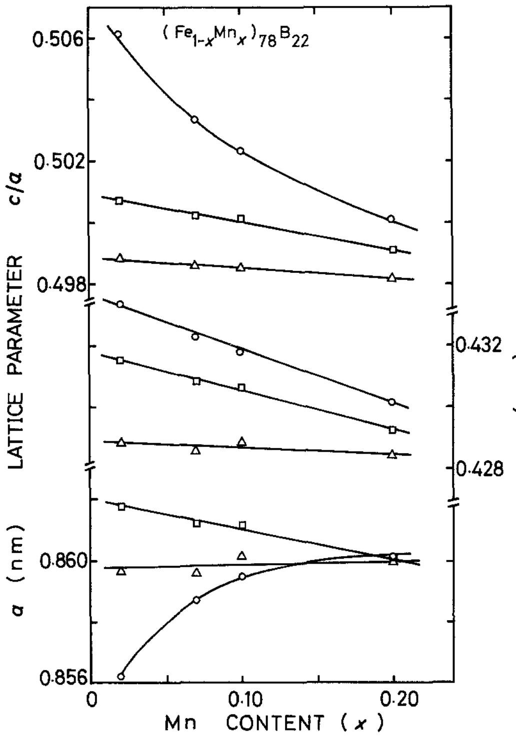

Figure 5 Dependence of lattice parameters *a*, *c* and *c/a* of the b c t $(FeMn)_3B$ phase on manganese concentration under three heat treatments. (○) 433 to 440° C, (△) 510 to 550° C, (□) 660° C, 5 h.

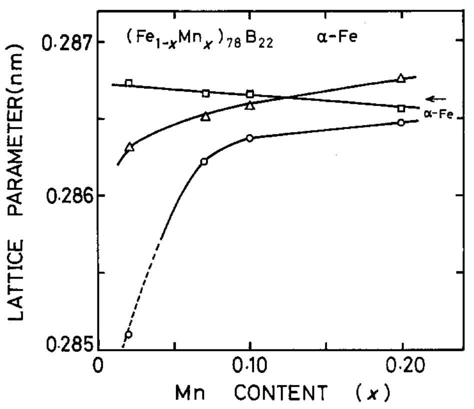

Figure 6 Variation of lattice parameter a of the α-Fe phase with manganese concentration and heat treatment. The horizontal arrow indicates the lattice parameter of pure α-Fe. (○) 433 to 444° C, (△) 510 to 550° C, (□) 660° C, 5 h.

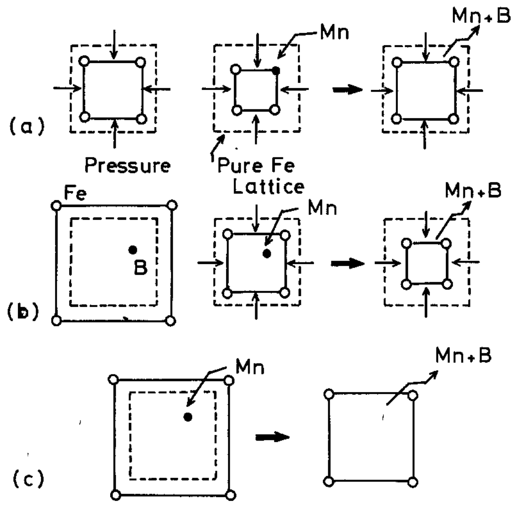

Figure 7 Schematic presentation of the change in lattice distance of α-Fe phase with pressure, the site of the occupying boron atom and chemical ordering between manganese and boron atoms, where the open circle represents the iron atom and the full circle the boron atom.

the amorphous state a chemical short range ordering between manganese and boron may be preferentially formed, because the manganese atom is slightly larger in atomic radius compared to the iron atom. Walter [11] concluded that addition of atoms of larger atomic radius to the $Fe_{82}B_{18}$ alloy leads to a higher crystallization temperature. Riontino and Marino [12] suggested a higher probability of clustering for manganese and boron atoms in terms of the measurement of isothermal variation of resistivity. As a result of the enhancement of the ordering with increasing manganese concentration, therefore, we can observe the obscure transition from the amorphous to the crystalline state, followed by a gradual change in resistance and the resistance minimum.

4.2. Structure analysis by X-ray diffraction

Initially we will discuss the crystalline state of the α-Fe phase. Samples heated to 433 to 440° C are normally believed to be a mixture of α-Fe, bct $(FeMn)_3B$ and amorphous phases. The influence on the α-Fe phase of pressure from the environment results in a contraction of the α-Fe lattice. The stress, p, is approximately represented by the equation $p = (\Delta a/a_{Fe})\,E$, where a_{Fe} is the lattice parameter of pure α-Fe, Δa the difference from a_{Fe}, and E Young's modulus. In a case of the manganese concentration of $x = 0.07$, for instance, $p = 2.2 \times 10^3$ atm (2.2×10^8 Pa) is obtained with $a_{Fe} = 0.28662$ nm, $\Delta a = 4.0 \times 10^{-4}$ nm and by using $E = 1.6 \times 10^{11}\,N\,m^{-2}$ for $Fe_{80}B_{20}$ alloy [13]. In the sample subjected to heating to 510 to 550° C, it is likely that the amorphous phase diminishes in population or hardly exists, leading to a decrease in stress and an expansion of the lattice. In fact, we obtain $p = 6.0 \times 10^2$ atm (6.0×10^7 Pa) with $\Delta a = 1.1 \times 10^{-4}$ nm for the same manganese concentration.

It is generally thought that super-saturated boron dissolves in the α-Fe phase, in substitutional or interstitial sites [14]. The variation of lattice parameter as seen in Fig. 6 will be qualitatively understood from the following discussion. In Fig. 7a, the behaviour of the lattice with pressure is schematically presented. The dashed and full lines represent the lattice of pure α-Fe, and the lattice which has contracted due to pressure from the environment, respectively. Provided that the boron atom substitutionally occupies the site, the lattice will be reduced still further, because of the smaller atomic size of the boron atom compared to that of the iron atom. This situation actually corresponds to the state heated to 433 to 440° C. In the samples heated to 510 to 550° C, the lattice expands because of a decrease in stress. If we assume chemical ordering between manganese and boron atoms and its enhancement with manganese concentration, an explanation may be given for the behaviour: the lattice approaches that of pure α-Fe in enriched manganese alloys, as a result of a decrease in the number of boron atoms in the α-Fe phase due to the chemical ordering.

Next in the case where the boron atom occupies interstitial site, the stress-free lattice may expand by the presence of the interstitial atom, as seen in Fig. 7b. The present data, however, indicate that the lattice should contact by the stress exerted from the environment at low manganese concentrations, independent of the existence of the interstitial atom. In a similar way of thinking, the lattice should diminish in size with manganese concentration as a result of a decrease in the population of boron atoms. This behaviour is inconsistent with the present manganese concentration dependence (Fig. 6). In the sample subjected to the heat treatments mentioned above, it follows that boron atoms occupy the α-Fe phase substitutionally, rather than interstitially.

In the interface between α-Fe and bct phases, the lattice is probably subjected to pressure or tensile stress influenced by the other phase [14]. The following reasons may be given for the lattice expansion of α-Fe in annealed samples: (1) the α-Fe lattice is subjected to tensile stress by the bct phase; (2) the boron atoms interstitially occupy the α-Fe lattice. However, an estimate can be made that the presence of interstitial boron atom, as claimed by Wang *et al.* [7] for the $Fe_{83}B_{17}$ alloy in equilibrium, mainly contributes to the lattice expansion, since the X-ray diffraction patterns of the α-Fe phase in Fig. 4 show that the sample annealed at 660° C for 5 h is nearly stress-free. To explain the behaviour of the annealed sample shown in Fig. 6, therefore, we must assume the presence of boron atom interstitially occupying the lattice, which has not been verified experimentally in this work, as shown in Fig. 7c.

On the other hand, this is not very simple for the bct $(FeMn)_3B$ phase, because the peak height of X-ray diffraction diminishes and other peaks existing on heating to 510 to 550° C, (6 1 1), (6 4 0), (0 0 4), (5 5 2), are not observed or are too weak to be identified, in annealed samples, as shown in Table I. As one possibility, a transformation from bct $(FeMn)_3B$ to bct $(FeMn)_2B$ is supposed. However, we can exclude this possibility on the grounds that the latter phase appears near 800° C [15] and its lattice parameter of the a-axis (0.51 nm) [16] is quite different from that of the present data (0.86 nm). There may be another possibility of the appearance of an orthorhombic $(FeMn)_3B$ phase. Since the diffraction lines of bct and orthorhombic phases are similar to each other [8], more discussion about this possibility cannot be now presented.

On the basis of the similar variation of lattice parameters of the a-axis in bct and α-Fe phases, it is possible that boron atoms occupy not only substitutionally but also interstitially in the bct phase with a large interatomic distance. However, the behaviour of the lattice parameter in the bct phase cannot be understood straightforwardly from solely the site the boron atoms occupy and the stress effect, just as in the α-Fe phase. Together with the chemical ordering between manganese and boron atoms, therefore, the effect of the increasing coupling between iron and manganese atoms with manganese concentration should be taken into account, which manifests itself in the change in the crystal structure factor due to the redistribution of α-Fe, manganese and boron atoms in the unit cell.

References

1. A. K. SINHA, *J. Appl. Phys.* **42** (1971) 338.
2. R. J. BIRGENEAU, J. A. TARVIN, G. SHIRANE, E. M. GYORGY, R. C. SHERWOOD, H. S. CHEN and C. L. CHIEN, *Phys. Rev. B.* **18** (1978) 2192.
3. H. ONODERA and H. YAMAMOTO, *J. Phys. Soc. Jpn* **50** (1981) 3575.
4. K. HEINEMANN and K. BÄRNER, *J. Magn. Magn. Mater.* **42** (1984) 291.
5. T. SOUMURA, K. TAKEDA, T. WAKANO, K. TERASAWA and T. MAEDA, *ibid* **58** (1986) 202.
6. U. HEROLD and U. KÖSTER, in "Proceedings of the 3rd International Conference on Rapidly Quenched Metals", Vol. 1, Brighton, July 1978, edited by B. Cantor (The Metals Society, London) p. 281.
7. W. K. WANG, H. IWASAKI and K. FUKAMICHI, *J. Mater. Sci.* **15** (1980) 2701.
8. M. TAKAHASHI, M. KOSHIMURA and T. ABUZUKA, *Jpn. J. Appl. Phys.* **20** (1981) 1821.
9. H. W. BERGMANN and U. BROKMEIER, "Rapidly Solidified Amorphous and Crystalline Alloys", edited by B. H. Kear, B. C. Giessen and M. Cohen (Elsevier, New York, 1982) p. 235.
10. A. LUCCI, G. RIONTINO, F. MARINO, C. ANTONIONE and G. COCCO, *Mater. Chem. Phys.* **10** (1984) 549.
11. J. L. WALTER, *Mater. Sci. Eng.* **50** (1981) 137.
12. G. RIONTINO and F. MARINO, *Scripta Metall.* **18** (1984) 13.
13. S. H. WHANG, D. E. POLK and B. C. GIESSEN, in "Proceedings of the 4th International Conference on Rapidly Quenched Metals, Vol. 11, Sendai 1981, edited by T. Masumoto and K. Suzuki (The Japan Institute of Metals, Sendai, 1982) p. 1365.
14. Y. MORIYA, H. ICHINOSE and H. INO, *Seisan-Kenkyu* **36** (1984) 30.
15. O. T. INAL, C. V. ROBINO, L. KELLER, F. G. YOST and M. M. KARNOWSKY, *J. Mater. Sci.* **16** (1981) 3183.
16. M. HANSEN (ed.) "Constitution of Binary Alloys" (McGraw-Hill, New York, 1958) p. 249.

Received 13 January
and accepted 13 March 1986